OPTIMIZATION OF MULTI-LAYER METALLIZATION DESIGN FOR LARGE-AREA BACK-CONTACT BACK-JUNCTION SOLAR CELLS

M. Hendrichs, R. Keding, A. Spribille, T. Fellmeth, S. Nold, F. Clement, A. Wolf, D. Biro
Fraunhofer Institute for Solar Energy Systems ISE, Heidenhofstraße 2, 79110 Freiburg, Germany
Phone: +49 761 - 4588 5074, e-mail: max-sebastian.hendrichs@ise.fraunhofer.de

ABSTRACT: In this study, a multi-layer metallization concept for high-efficient large-area silicon back-contact back-junction solar cells is investigated. The metallization approach represents an industrial alternative to the well-known edge-to-edge cell interconnection technology, allowing for a decoupling of the cell metallization from the external contact structure by inserting an intermediate insulation layer. A first proof of principle is shown for an n-type back-contact back-junction solar cell with an edge length of 156 mm and evaporated aluminum grid fingers. Furthermore, we present a tool that allows for the design optimization of the contact layout by combining detailed cost of ownership calculations with analytical solar cell simulations. Two back-end process sequences are compared and for both approaches the most cost-effective metallization layout is determined on cell level. Finally, a sensitivity analysis is carried out, revealing the high potential of the investigated back-contact back junction solar cell structures.
Keywords: back contact, cost reduction, metallization, modelling, solar cell

1 INTRODUCTION

The recently published conversion efficiency record of 25.6 % [1] for n-type silicon back-contact back-junction (BC-BJ) solar cells emphasizes their superior conversion efficiency potential. Not only on laboratory scale but also in industrial environment high conversion efficiencies have been shown so far on cell and module level [2]. Up to now most BC-BJ solar cells in industry and research feature a so called interdigitated back contact (IBC) metallization pattern (see Fig. 1a), where the external p-type and n-type contacts are each located at opposed wafer edges. In order to keep resistive losses within the IBC structure on an acceptable level, it is either necessary to increase the finger cross section or to reduce the lateral current path in the contact fingers. The IBC geometry is probably the main reason why most of today's BC-BJ solar cells are fabricated using silicon wafers with an edge length of 125 mm, which are metallized with technologies allowing for high aspect ratios, as for example plating or comparable.

In order to adopt the BC-BJ cell concept i) to an industrial wafer format with 156 mm edge length and ii) to cost-effective finger metallization technologies as for instance screen printing, alternative metallization concepts are essential. In this work we investigate a multi-layer metallization concept for BC-BJ solar cells [3–6] that allows for a flexible placing of the external contacts within the cell area, hence reducing current paths in the contact grid of BC-BJ solar cells with 156 mm edge length (see Fig. 1b). Furthermore, it enables the usage of conventional equipment for back-contact current-voltage (*I-V*) measurements to characterize BC-BJ solar cells. A first proof of principle is shown on cell level. In addition, we present a simulation tool that allows for design optimization of the multi-layer metallization concept. Numerical simulations are coupled with cost of owner ship (CoO) calculations in order to find the most cost-effective metallization layout for different finger metallization technologies.

2 APPROACH

2.1 Multi-layer metallization concept

The BC-BJ multi-layer cell metallization concept is depicted in Fig. 2. It consists of three layers: a) contact finger grid, b) screen-printed insulating layer and c) screen-printed busbar metallization. The external p-type and n-type busbar contacts are decoupled from the cell metallization by an intermediate insulation layer, thus opening up an extensive range of contact layouts to choose from. In this study, we use a thermally cured solder resist as insulation paste and a commercial copper-based low-temperature conductive paste as busbar metallization. Both materials are applied by conventional screen printing, allowing for an easy integration of the multi-layer metallization concept in state of the art cell production facilities.

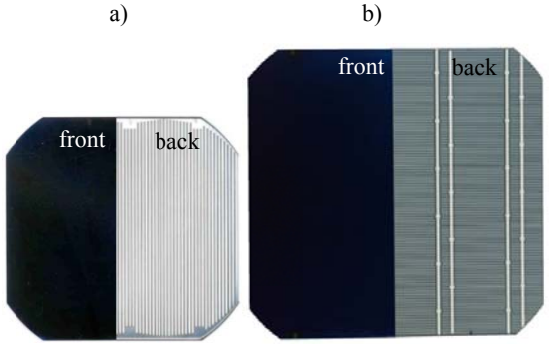

Figure 1: Front and back side of a BC-BJ solar with a) interdigitated back contact (IBC) metallization pattern and an edge length of 125 mm and b) with four busbar multi-layer metallization and an edge length of 156 mm.

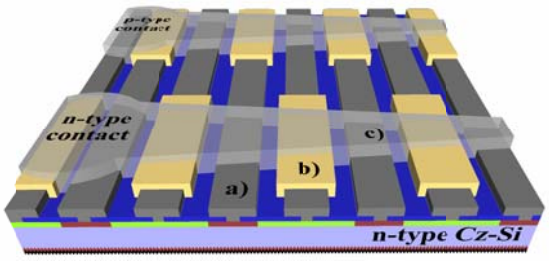

Figure 2: Schematic cross section of the investigated n-type BC-BJ multi-layer metallization concept consisting of a) contact finger grid, b) insulating layer and c) busbar metallization.

2.2 Cell fabrication

Large-area BC-BJ solar cells with multi-layer metallization were fabricated using n-type Czochralski-grown silicon (Cz-Si) wafers with a base resistivity of 3 Ωcm and an edge length of 156 mm. The base line process described in [7,8] was used. All doped layers were formed during a single high-temperature step using silicate glasses as doping sources. The cell design features a pitch of 1.5 mm and a back surface field (BSF) width of 300 µm. After passivation and local contact opening the cells were full-area metallized with a 4.5 µm thick evaporated aluminum layer [9]. The aluminum layer was structured, resulting in 140 µm wide n-type contact fingers and 490 µm wide p-type contact fingers. A thermal curing solder resist was screen printed on the patterned aluminum layer insulating every second metal finger. Finally the low-temperature copper-based busbar paste was screen printed in form of a three busbar layout.

3 RESULTS AND DISCUSSION

3.1 Experimental results

The *I-V* characteristics of the BC-BJ cell with the best performance so far is shown in Table 1. Short-circuit current j_{SC} and open-circuit voltage V_{OC} are limited due to process difficulties in the front-end which have been overcome recently, see [8]. The pseudo fill factor *pFF* indicates that the multi-layer metallization approach was implemented successfully without significant shunt contributions.

Table I: *I-V* data of the best performing n-type Cz-Si BC-BJ solar cell with a three-busbar multi-layer metallization and 156 mm edge length, *A* with an active cell area of 239 cm² and *B* with isolated edges and an active cell area of 216 cm². The cell was measured with an industrial cell tester under standard test conditions.

	V_{OC} (mV)	j_{SC} (mA/cm²)	*FF* (%)	*pFF* (%)	R_S (Ωcm²)	η (%)
A	630.1	37.7	76.2	82.0	1.1	18.1
B	630.8	38.1	77.2	81.9	0.9	18.6

The resistive loss within the multi-layer metallization $R_{S,met}$ including the evaporated aluminum finger is calculated as follows:

$$R_{S,met} = \frac{1}{12} R_{BB} \frac{A_{cell}}{n_{BB}} \quad (1)$$

with R_{BB} the measured resistance between two busbars of one polarity, A_{cell} the active solar cell area and n_{BB} the number of busbars per polarity. For the full-area measurement $R_{S,met} = 0.3$ Ωcm² is calculated, corresponding to approximately one third of the total fill factor loss. The series resistance contribution of the multi-layer metallization approach proves the low contact resistance between the evaporated aluminum finger grid and the low-temperature busbar paste. The cell result can be understood as a first proof of principle of the multi-layer metallization approach and shows the basic functionality of the concept with evaporated aluminum grid fingers without capping layer.

3.2 Device simulation and cost of ownership calculation

As the investigated multi-layer metallization approach offers a wide range of possible BC-BJ contact designs, the question arises, which pad layout is most cost-effective for 156 mm BC-BJ solar cells. In order to answer this question on solar cell level, we present a design optimization procedure based on numerical cell simulations coupled with *SCost* [10], a bottom-up cost of ownership calculation tool, varying the number of busbars and the number of pads per busbar systematically.

a)

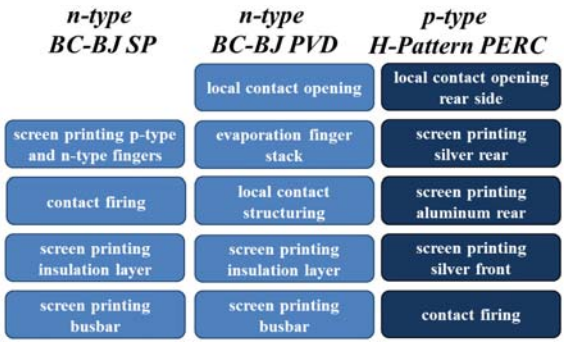

b)

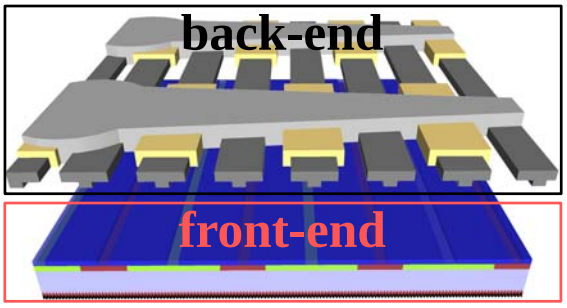

Figure 3: a) Investigated back-end process sequences for n-type BC-BJ solar cells with an edge length of 156 mm. As reference a conventional p-type H-pattern solar cell with passivated emitter and rear cell (PERC) and b) Schematic drawing of the classification in front-end and back-end for the BC-BJ solar cell analysis presented in this study.

For the BC-BJ solar cell analysis, two different back-end process sequences are compared: one with evaporated (BC-BJ PVD) and the other one with screen-printed (BC-BJ SP) finger metallization, see Fig. 3a. The back-end fabrication starts with a fully passivated cell precursor, as depicted in Fig. 3b. For the front-end, the process sequence investigated in [11] with an ion-implanted BSF structure and a boron-doped front floating emitter is assumed. The rear passivation layer is considered to provide electrical insulation between finger metallization and doped areas. As a reference, we include the state of the art screen-printed three-busbar p-type Cz-Si H-pattern solar cell with passivated emitter and rear cell (PERC) from [12,13] in our calculations.

The BC-BJ solar cell simulation tool allows to calculate all resistive losses in the metallization layers, the doped areas and the base of 156 mm full-square 1 Ωcm n-type Cz-Si BC-BJ solar cells using analytical equations. All relevant *I-V* parameters are simulated applying the one-diode model. As a basis, the dark saturation current densites j_0 from literature shown in Table 2 are used. Note that reference for the $j_{0E,met}$ of the BC-BJ SP approach was determined for a silver-

aluminum paste, usually used for the front metallization of n-type H-pattern solar cells. This value must be understood as a rough estimation, since up to now no j_0 measurements were carried out for the silver paste investigated in this work. The parallel resistance R_P is assumed to be 10 kΩcm² and the photo current density 41 mA/cm². For all investigated BC-BJ solar cells a finger pitch of 1.5 mm and a BSF width of 300 µm without gap between emitter and BSF are assumed. All metallization related simulation parameters are depicted in Table 3.

Table II: Dark saturation current densities j_0 from literature used as input parameters for the one- diode model.

j_0 current type	BC-BJ SP	BC-BJ PVD
j_{0bulk} (fA/cm²)	30 [14]	30 [14]
j_{0FFE} (fA/cm²)	40 [11]	40 [11]
j_{0BSF} (fA/cm²)	300 [15]	300 [15]
j_{0E} (fA/cm²)	20 [11]	20 [11]
$j_{0E,met}$ (fA/cm²)	3000 [16]	1500 [11]
$j_{0BSF,met}$ (fA/cm²)	1500 [17]	700 [11]
j_{0total} (fA/cm²)	**257**	**181**

Table III: Metallization related input parameters for all investigated solar cell technologies.

	BC-BJ SP	BC-BJ PVD	H-pattern PERC
finger width (µm)	50	710	50
effective finger height (µm)	11	1.5	11
finger resistivity (µΩcm)	3.5	3.1	3.5
contact resistivity of finger grid ρ_C (mΩcm²)	8	1	3
finger mass (mg)	97 (Ag)	98 (Al)	80 (Ag)
busbar resistivity (µΩcm)	35	35	3.5
contact resistivity busbar to finger (µΩcm²)	10	10	0
mass busbar (mg)	66-163*	59-162*	20

*depending on number of busbars, see Fig 4.

For the BC-BJ SP solar cells both emitter and BSF are contacted with the same commercial firing-through silver paste in a single screen printing step. Measurements using the transfer length method (TLM) [18] reveal a contact resistivity of about 8 mΩcm² for this paste on both polarities. The finger width is simulated with 50 µm for all contact fingers.

In case of the BC-BJ PVD solar cells a laser process is assumed for the local passivation ablation resulting in 50 µm wide linear contact openings. The evaporated fingers consist of 1.5 µm aluminum, 100 nm titanium nitride (TiN), 20 nm titanium (Ti) and 50 nm silver (Ag) layer stack deposited in one industrial evaporation tool [9]. The TiN/Ti/Ag layer stack provides an effective aluminum diffusion barrier, hence enabling the long-term stability of the metal contact system [19]. For the finger structuring technology, the direct ink-jet etching process investigated in [20] is assumed. A reduced process sequence is analyzed with the BC-BJ PVD* approach that features solely the 1.5 µm thick aluminum layer without capping, hence representing the fabrication concept shown in section 2.2.

For both BC-BJ back-end process sequences a measured value of 10 µΩcm² is applied for the contact resistivity between copper-based low-temperature busbar paste and grid metallization. The round external contact pads measure 2 mm in diameter. The tapering of the busbar between the solder pads is cost-optimized for all investigated metallization layouts using an analytical simulation tool applying a minimum busbar width of 100 µm and a maximum width of 2000 µm. Note that no bifaciality factor is taken into account for the simulated BC-BJ solar cells.

Fig. 4a shows the simulated solar cell conversion efficiencies for all investigated metallization layouts. The BC-BJ PVD solar cells reach maximum conversion efficiencies over 22.5 % for metallization layouts with more than 5 busbars and 15 external contact pads per busbar. The conversion efficiency advantage of about 1 % absolute over the best BC-BJ SP cells results on the one hand from a 10 mV higher V_{OC} due to lower j_{0met} values and on the other hand from lower series resistance r_S values. The BC-BJ SP solar cells achieve minimum r_S of 0.7 Ωcm² whereas the BC-BJ PVD solar cells show $r_S < 0.4$ Ωcm². This gap is mainly caused by higher series resistance contributions of the electrical metal-semiconductor contact of the finger grid and the electrical

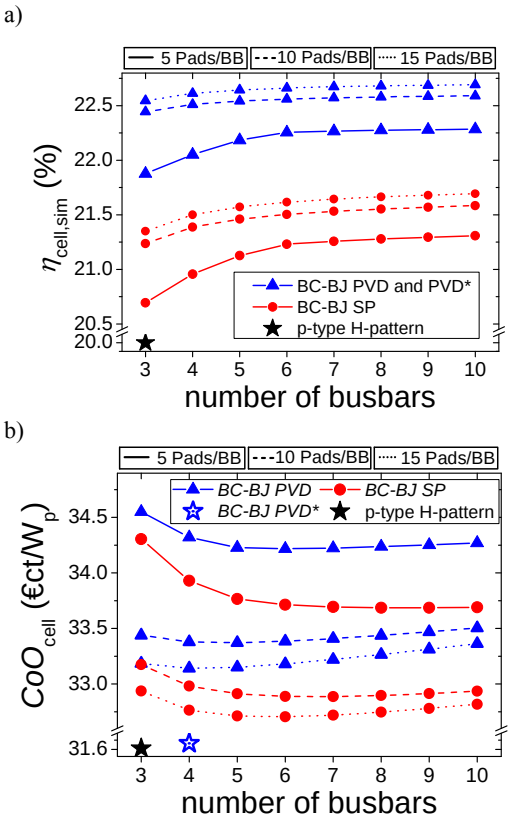

Figure 4: a) Simulated cell conversion efficiencies $\eta_{cell,sim}$ for large-area n-type Cz-Si BC-BJ solar cells with different back-end process and metallization layouts and b) Calculated cost of ownership (CoO_{cell}) for the simulated BC-BJ solar cells from Fig. 4a. The open star represents a BC-BJ PVD* solar cell without titanium nitride/titanium/silver capping for the finger metallization. The black star represents a state of the art p-type Cz-Si H-pattern PERC solar cell with screen-printed contacts.

contact between busbar and finger paste due to the reduced contact area in case of the BC-BJ SP solar cells.

The resulting CoO of all metallization layouts is shown in Fig. 4b calculated for a 500 MW_p production facility located in Europe and an amortization period of 7 years for equipment and 20 years for buildings. The as-cut silcon wafer costs are included with 94 €ct and 107 €ct per wafer for p-type and n-type silicon, respectively [21]. The front-end precursor is calculated with a cost of 41 €ct per wafer. The width of the solder resist stripe is 5 mm with an expected material price of 20 €/kg. For the busbar paste, a price of 350 €/kg is assumed. The cost of the firing-through silver paste for the finger metallization of the BC-BJ SP solar cells is based on the current silver price of 14.8 € per fine ounce.

A four busbar metallization layout with more than 10 pads per busbar is found to be most cost-effective for the simulated BC-BJ PVD solar cells. In case of the BC-BJ SP solar cells, the optimal metallization layout features five or more busbars with over 10 pads per busbar. Due to the reduced back-end process sequence (see Fig. 3) the BC-BJ SP solar cells achieve 1.5 % lower CoO in comparison to the BC-BJ PVD cells. Still, the best-case BC-BJ SP solar cells show about 4.5 % higher CoO compared with the conventional p-type H-Pattern PERC cell technology. The lowest BC-BJ CoO is achieved with the simplified BC-BJ PVD* approach that corresponds to the experimentally realized metallization structure shown in section 2.2. By omitting the TiN/Ti/Ag barrier stack a cost reduction of 4 % is calculated. Currently, the long-term stability of the BC-BJ PVD* metal contact system is investigated. The results will show, whether this approach not only provides a huge potential for cost reduction but also is industrially feasible.

a)

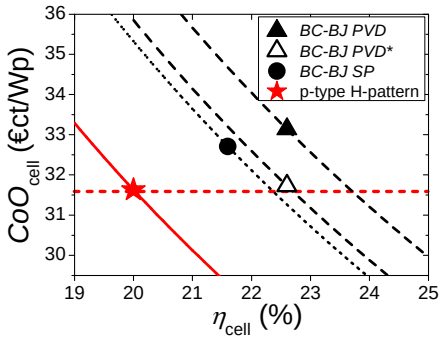

b)

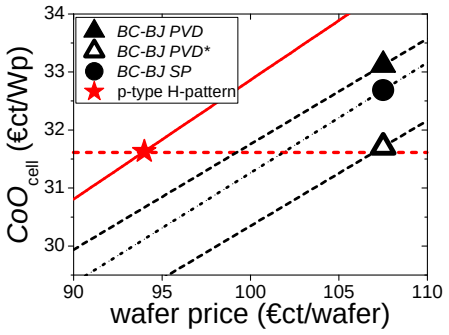

Figure 5: a) Sensitivity analysis of the solar cell conversion efficiency for the most cost-effective BC-BJ solar cells from Fig. 4 and b) Sensitivity analysis of the as-cut Cz-Si wafer price for the most cost-effective BC-BJ solar cells from Fig. 4. The black star represents the state of the art p-type Cz-Si H-pattern PERC solar cell with screen-printed contacts.

In order to estimate the future development of industrial BC-BJ solar cells a sensitivity analysis of the cell conversion efficiency and the n-type wafer price is carried out for the most cost-effective BC-BJ metallization layouts. Fig. 5a shows the sensitivity of the solar cell conversion efficiency for the presented simulation data. The CoO of the investigated large-area industrial BC-BJ solar cells is compatible with the conventional p-type PERC technology when the cell conversion efficiency reaches values over 22.4 % in case of screen-printed (BC-BJ SP) and 23.8 % in case of evaporated grid metallization (BC-BJ PVD and BC-BJ PVD*). In order to obtain this high conversion efficiency level the main research focus is the further reduction of dark saturation current densities. In case of the BC-BJ SP technology a huge improvement potential for the future remains in the optimization of the firing-through silver paste for the grid metallization. The main focus is reducing j_{0met} as well as contact resistivity of the finger grid ρ_C. Simulating the BC-BJ SP cell with $j_{0E,met}$ = 1000 fA/cm² and ρ_C = 3 mΩcm² results in $\eta_{cell,sim}$ = 22.3 %, clarifying the big influence of the finger paste.

Note that the p-type PERC technology is currently under further development and should therefore being understood as a moving target. The sensitivity analysis of the as-cut wafer price (Fig. 5b) reveals the strong influence of the base material cost for industrial BC-BJ solar cells. At present, the Cz-Si n-type wafer price is about 14% higher compared to p-type material. A reduction of the n-type silicon below 100 €ct/wafer facilitates the cost-competiveness of high efficiency n-type solar cells.

Finally it must not be forgotten that at the end the CoO on module and system level determine whether a new technology is suitable for market launch. High efficiency solar cells clearly gain CoO benefits on system level, since all area-proportional costs are used more efficiently [10]. Furthermore, in case of the BC-BJ solar technology the uniform cell and module appearance is an additional factor that could increase the future market share of BC-BJ solar cells.

4 CONCLUSIONS

We show a first experimental proof of principle of a multi-layer metallization concept for BC-BJ solar cells with an edge length of 156 mm and all-aluminum evaporated grid finger metallization. The results reveal the successful implementation of the metallization approach using an innovative and cost-effective copper-based conductive paste for the busbar metallization.

By means of analytical solar cell simulations combined with cost of ownership calculations a metallization layout optimization tool for industrial large-area n-type BC-BJ solar cells is presented. BC-BJ metallization layouts with minimum four busbars and more than 10 contact pads per busbar are found to be most cost-effective for both investigated grid finger metallization technologies – namely screen printing and physical vapor deposition.

Furthermore, we show that with the current base material price structure, n-type solar cells hardly gain cost advantages over the mature p-type technology on cell level. Only with high efficiency solar cell concepts with a conversion efficiency potential of more than 22 % cost benefits are feasible. For the BC-BJ solar cell with screen-printed grid metallization the highest potential for improvement lies in the development of metallization pastes with low j_{0met} and contact resistivity on p-type as well as on n-type doped areas. First commercial products are currently available and under further development. In case of the BC-BJ cell structure with evaporated finger grid, one of the most important questions is the necessity of the evaporated capping layers, which is found to be among the biggest cost drivers of this technology. First experimental results proof the feasibility of the multi-layer metallization concept without additional barrier layer stack. Our future investigations will focus on the confirmation of the long-term stability of this simplified metallization approach.

ACKNOWLEDGEMENTS

The authors thank all colleagues at the Fraunhofer ISE Photovoltaic Technology Evaluation Center (PV-TEC) for their support; especially M. Linke, E. Lohmüller, S. Werner, M. Jahn and V. Krumm. The work was supported by the European Union's Seventh Programme for research, technological development and demonstration under grant agreement No 608498.

REFERENCES

[1] Keiichiro Masuko et al., "Achievement of more than 25% conversion efficiency with crystalline silicon heterojunction solar cell", *Proc. 40th IEEE Photovoltaic Specialists Conference*, 2014.

[2] Smith, D. D. et al., "SunPower's Maxeon Gen III solar cell: high efficiency and energy yield", *Proc. 39th IEEE Photovoltaic Specialists Conference*, 2013.

[3] Halm, A. et al., "Evaluation of cell to module losses for n-type IBC solar cells assembled with state of the art consumables and production equipment", *Proc. 39th IEEE Photovoltaic Specialists Conference*, 2013.

[4] DeVecchi, S. et al., "New metallization scheme for interdigitated back contact silicon heterojunction solar cells", *Proc. SiliconPV*, 2013.

[5] Lammert, M. D. et al., "The interdigitated back contact solar cell: a silicon solar cell for use in concentrated sunlight", *IEEE Transactions on Electron Devices*, 1977.

[6] Galbiati, G. et al., "Large-Area Back-Contact Back-Junction Solar Cell With Efficiency Exceeding 21%", *Journal of Photovoltaics*, 2012.

[7] Keding, R. et al., "Co-Diffused back-Contact Back-Junction Silicon Solar Cells", *Proc. 28th EU-PVSEC*, 2013.

[8] Keding, R. et al., "POCL3-Based Co-Diffusion Process for n-type Back-Contact Back-Junction Solar Cells", *Proc. 29th EU-PVSEC*, 2014.

[9] Nekarda, J. et al., "Industrial PVD metallization for high efficiency crystalline silicon solar cells", *Proc. 34th IEEE Photovoltaic Specialists Conference*, 2009.

[10] Nold, S. et al., "Cost Modelling of Silicon Solar Cell Production Innovation Along the PV Value Chain", *Proc. 27th EU-PVSEC*, pp. 1084–1090, 2012.

[11] Müller, R. et al., "Back-junction back-contact n-type silicon solar cell with diffused boron emitter locally blocked by implanted phosphorus"", *Applied Physics Letters*, no. 105, 2014.

[12] Müller, J. W. et al., "Current status of q.cells' high-efficiency q.antum technology with new world record module results", *Proc. 27th EU-PVSEC*, vol. 2012 ,

[13] Xia, Z. et al., "Rear side dielectrics choices in PERC solar cells", *Proc. 39th IEEE Photovoltaic Specialists Conference*, 2013.

[14] Swanson, R. W. et al., "High-efficiency n-type", *Advances in solar energy*, 1990.

[15] A. Lanterne, S. Gall, S. Manuel et al., "Annealing, Passivation and Contacting of Ion Implanted Phosphorus Emitter Solar Cells", *Energy Procedia*, vol. 27, pp. 580–585, 2012.

[16] Geerligs, L. J. et al., "Progress in low-cost n-type silicon solar cell technology", *Proc. 38th IEEE Photovoltaic Specialists Conference*, 2012.

[17] Fellmeth, T. et al., "Recombination at metal-emitter interfaces of front contact technologies for highly efficient silicon solar cells", *Proc. SiliconPV*, 2008.

[18] H. H. Berger, "Contact resistance and contact resistivity", *J. Electrochem. Soc.*, vol. 119, no. 4, pp. 507–514, 1972.

[19] Nekarda, J. et al., "Industrial inline PVD metallization for silicon solar cells with laser fired contacts leading to 21.8 % efficiency", *2nd workshop on metallization*, 2010.

[20] Kumm, J. et al., "Development of temperature-stable, solderable PVD rear metallization for industrial silicon solar cells", *Proc. 28th EU-PVSEC*, 2013.

[21] Stuewe, D. et al., "Etching of PVD Metal Layers for Contact Separation of Back Contact Silicon Solar Cells using Inkjet-Printing", *NIP & Digital Fabrication Conference*, 2013.

[22] www.pv-insight.com, 2014.